Since January 2020 Elsevier has created a COVID-19 resource centre with free information in English and Mandarin on the novel coronavirus COVID-19. The COVID-19 resource centre is hosted on Elsevier Connect, the company's public news and information website.

Epidemics 40 (2022) 100617

Contents lists available at ScienceDirect

Epidemics

journal homepage: www.elsevier.com/locate/epidemics

Estimating transmission dynamics of SARS-CoV-2 at different intraspatial levels in an institutional outbreak

Shihui Jin [a,b], Borame Lee Dickens [a], Amy ML Quek [c,d], Mikael Hartman [a,e], Paul Anantharajah Tambyah [c], Raymond Chee Seong Seet [c,d], Alex R. Cook [a,b,*]

[a] Saw Swee Hock School of Public Health, National University of Singapore and National University Health System, Singapore
[b] Department of Statistics and Data Science, National University of Singapore, Singapore
[c] Department of Medicine, Yong Loo Lin School of Medicine, National University of Singapore, Singapore
[d] Division of Neurology, Department of Medicine, National University Hospital, Singapore
[e] Department of Surgery, National University of Singapore, Singapore

ARTICLE INFO

Keywords:
Data augmentation
Transmission dynamics
Outbreak modelling
Migrant workers
SARS-CoV-2

ABSTRACT

Introduction: Large, localised outbreaks of COVID-19 have been repeatedly reported in high-density residential institutions. Understanding the transmission dynamics will inform outbreak response and the design of living environments that are more resilient to future outbreaks.
Methods: We developed an individual-based, multilevel transmission dynamics model using case, serology and symptom data from a 60-day cluster randomised trial of prophylaxes in a densely populated foreign worker dormitory in Singapore. Using Bayesian data augmentation, we estimated the basic reproduction number and the contribution that within-room, between-level and across-block transmission made to it, and the prevalence of infection over the study period across different spatial levels. We then simulated the impact of changing the building layouts in terms of floors and blocks on outbreak size.
Results: We found that the basic reproduction number was 2.76 averaged over the different putative prophylaxes, with substantial contributions due to transmission beyond the residents' rooms. By the end of ~60 days of follow up, prevalence was 64.4 % (95 % credible interval 64.2–64.6 %). Future outbreak sizes could feasibly be halved by reducing the density to include additional housing blocks, or taller buildings, while retaining the overall number of men in the complex.
Discussion: The methods discussed can potentially be utilised to estimate transmission dynamics at any high-density accommodation site with the availability of case and serology data. The restructuring of infrastructure to reduce the number of residents per room can dramatically slow down epidemics, and therefore should be considered by policymakers as a long-term intervention.

1. Introduction

The COVID-19 pandemic has disproportionately affected the most vulnerable groups in society: low-income communities, racial minorities, the homeless, those in institutional housing and migrants (Shadmi et al., 2020; Team and Manderson, 2020). Migrant workers experience a confluence of vulnerabilities: they are often lower-income, sometimes ethnic minorities, often do work that cannot be done remotely, may have a precarious legal or residential status, and are more likely to live in crowded housing. Large outbreaks among migrant worker communities have been observed in Kuwait (Alali et al., 2021), Singapore (Gorny et al., 2021) and Thailand (Rojanaworarit and Bouzaidi, 2021).

Singapore was one of the first countries outside China to identify COVID-19 cases and, despite early successes in containing spread among the general population, experienced rampant transmission among migrant workers living in purpose-built and other dormitories. The affected community was mostly men working in manual or technical roles, typically aged 20–55, living in high density accommodation with 10–20 men per room and thousands of men per dormitory (Gorny et al., 2021; Rojanaworarit and Bouzaidi, 2021; Koh, 2020). From mid-April, 2020, the government implemented strict containment measures, imposing *cordons sanitaires* on dormitories to prevent residents' entry

* Correspondence to: #10-01 Tahir Foundation Building, 12 Science Drive 2, 117549, Singapore.
E-mail address: ephcar@nus.edu.sg (A.R. Cook).

https://doi.org/10.1016/j.epidem.2022.100617
Received 9 February 2022; Received in revised form 8 July 2022; Accepted 20 July 2022
Available online 22 July 2022

and exit and further movement restrictions within dormitories, measures which were partially relaxed from July, as the outbreak came under control and the residents resumed work, albeit with restrictions to their liberties that persisted over a year thereafter. Despite the efforts to contain spread, the prevalence of PCR or serology confirmed infection among migrant workers living in dormitories in Singapore reached 56 % by August 2020 (Tan et al., 2021), highlighting the vulnerability of this group.

Dormitory residents are at great risk of infection due to the high density of their accommodation (Sadarangani et al., 2017). The sharing of facilities such as toilets, showers and kitchens, as well as sleeping spaces, facilitates transmission via the inhalation of respiratory particles due to the close proximity and direct contact with respiratory tract secretions or other infectious body fluids of infected persons (Franco-Paredes et al., 2020). Although structural accommodation changes are underway, very many migrant workers in Singapore will continue to share spaces in highly populated settings (Yi et al., 2021). This is particularly of concern with the global, rapid rise of the delta and then omicron variants (Chia et al., 2021; Pulliam et al., 2021), and the re-emergence of dormitory clusters in Singapore (COVID-19 Situation Report, 2021), which make understanding the localised epidemic critical.

Gaining quantitative understanding on the transmission dynamics and evaluating the effects of building layout within such high-density settings will be advantageous in restructuring living and working arrangements, and prospectively redesigning dormitories, to mitigate the impact of future outbreaks. Utilising collected data on seroprevalence and symptom onset for 4257 residents at a foreign worker dormitory from May to July 2020 as part of a prophylaxis trial (Seet et al., 2021), this paper has two aims: firstly to infer infection progression through space and time, and thereby to estimate the basic reproduction number (R_0) and the contributions to it that different intraspatial levels made, including within room, between levels and across blocks. This was achieved using a Bayesian data augmentation approach of an individual-level disease state model. Secondly, we simulated epidemics based on the estimated transmission rates across a range of different building configurations to determine how changes in the number of floors and housing blocks affects outbreak size.

2. Materials and methods

2.1. Population under study

The data collated for this study were obtained from a 60-day (May 19 to July 17, 2020) cluster randomized trial at Tuas South Dormitory, a dormitory for male migrant workers in western Singapore comprising five 9-floor residential blocks with similar floor plans. Each block has one staircase and one elevator for all the residents to share, and each floor has 14 units designed to maximally accommodate either 12 or 16 persons (Fig. S1). *En suite* toilets and shower facilities are available in all the units as well. The first case of COVID-19 in the dormitory was identified on April 7, 2020, 16 days before it was gazetted as an isolation area which meant all individuals, including but not limited to the dormitory residents, were unallowed to enter or exit the premises except for medical reasons, and intermingling among individuals on site was strictly minimised. Mask wearing was mandated but was monitored only in public areas and thus compliance might not have been complete. In all, 4257 out of the 6502 dormitory residents met the eligibility criteria and consented to participate in the trial, which aimed to determine whether any of oral hydroxychloroquine, oral ivermectin, povidone-iodine throat spray, oral zinc/vitamin C combination and oral vitamin C could serve as prophylaxis. Participants provided informed consented in their own languages after an extended process of explanation and the trial was approved by the Domain-Specific Review Board, National Healthcare Group (2020/00561), the Ministry of Health, the multi-ministerial Joint Task Force, and was conducted under a Clinical Trial Authorization (CTA2000053) by the Health Sciences Authority, which oversees all clinical trials in Singapore. The main results have been published elsewhere (Seet et al., 2021).

2.2. Serology and case data

Two rounds of SARS-CoV-2 antibody tests were conducted in the trial. The first took place upon enrollment within the first 17 days of the study, from May 19 to June 4, 2020, while the second was targeted at 42 days after the first, from June 29 to July 14, 2020. Among the workers who enrolled in the study, all but 6 (99.9 %) had the first antibody test, among whom 456 (10.7 %) tested positive indicating they had been infected before the trial started. By the time of the second test, which involved all but 19 (99.6 %) men, 2586 (60.8 %) were positive, i.e. 2131 (50.0 %) men seroconverted over the course of the six weeks in the trial (Table 1).

A total of 401 (9.4 %) participants received a reverse transcription polymerase chain reaction ([RT-]PCR) test after they or their roommates developed respiratory symptoms during the study. Asymptomatic individuals were not tested unless they were identified as close contacts of a symptomatic case who was PCR positive. Only 2 (2.1 %) of the tested individuals obtained a negative result. For those who were PCR positive, we imputed a seropositive result in the second serology test regardless of the actual test result.

2.3. Symptom data

Self-reported data of 23 associated symptoms and the time of development were collected via an online platform from a total of 4054 residents of the dormitory. According to the serology test results, among those who provided results, 2017 (49.8 %) became infected during the study of whom 510 (25.3 %) declared that they had experienced at least one of the 23 symptoms during the trial.

2.4. Modelling framework

We created three submodels specifically addressing symptom profiles, infection size and infection rate, illustrated in Fig. 1 and described below.

2.4.1. Model of symptoms

Appearance rates of the 23 symptoms between the infected and uninfected populations were compared and we included seven in the model including fever, cough, runny nose, sore throat, change in smell, change in taste and loss of appetite, since these discriminated the infected and uninfected residents well (**SI** Fig. S3). In this model, we only considered symptomatic individuals who became infected during the study period of May 19 to July 17, 2020, i.e. those who were tested negative in the first serology test but positive in the second, and showed at least one of the seven of symptoms between the two tests.

For individual i infected at time T^i_{inf}, the number of symptoms among the septet reported on day t after infection, $N^i(t + T^i_{inf})$, is assumed to follow a beta-binomial distribution with mean $\mu(t) = 7a_3 f_{a_1,a_2}(t)$ and variance $\nu(t) = \theta\mu(t)$, where $f_{a,b}(x)$ is the probability density function of the log-normal distribution $LN\left(a, b^2\right)$. In this model, a_1, a_2, a_3 and θ are time invariant parameters to be estimated, i.e.

$$N^i\left(t + T^i_{inf}\right) \sim \mathrm{Bin}\left(7, p^i(t)\right),$$

$$p^i(t) \sim \mathrm{Beta}(\alpha(t), \beta(t)),$$

where $\alpha(t) = \mu(t)\left[\frac{1-\mu(t)}{\theta} - 1\right]$ and $\beta(t) = [1-\mu(t)]\left[\frac{1-\mu(t)}{\theta} - 1\right]$ such that $\mathbb{E}p^i(t) = \frac{\alpha(t)}{\alpha(t)+\beta(t)} = \mu(t)$. Under this model, $\mathbf{P}\left(N^i\left(t + T^i_{inf}\right) = 0\right) =$

Table 1
Number and proportion of COVID-19 cases with positive serology test results, seroconversions, and symptomatic and asymptomatic infections among the 4257 participants at Tuas South Dormitory over the period of May 19 to July 17, 2020. Symptomatic infections at follow up requires an initial negative serology test and a positive result during the follow up period with the presentation of at least one of seven symptoms between the two tests (fever, cough, runny nose, sore throat, change in smell, change in taste and loss of appetite).

Block No.	No. Floors	No. Rooms	No. of Residents	Seropositives at beginning	Seropositives after $\Delta t = 42$ days	Seroconversions from $t = 0$ to $t = 60$	Symptomatic at time of follow up	Asymptomatic at time of follow up
5	5	63	589	28 (4 %)	334 (57 %)	306 (52 %)	50 (16 %)	256 (84 %)
7	8	100	876	164 (19 %)	581 (66 %)	417 (48 %)	46 (11 %)	371 (89 %)
9	9	112	900	98 (11 %)	693 (77 %)	595 (66 %)	106 (18 %)	489 (82 %)
11	9	99	855	123 (14 %)	323 (38 %)	200 (23 %)	27 (13 %)	173 (87 %)
13	9	113	1037	43 (4 %)	659 (64 %)	616 (59 %)	99 (16 %)	517 (84 %)
Total	40	487	4257	456 (11 %)	2590 (61 %)	2134 (50 %)	328 (15 %)	1806 (85 %)

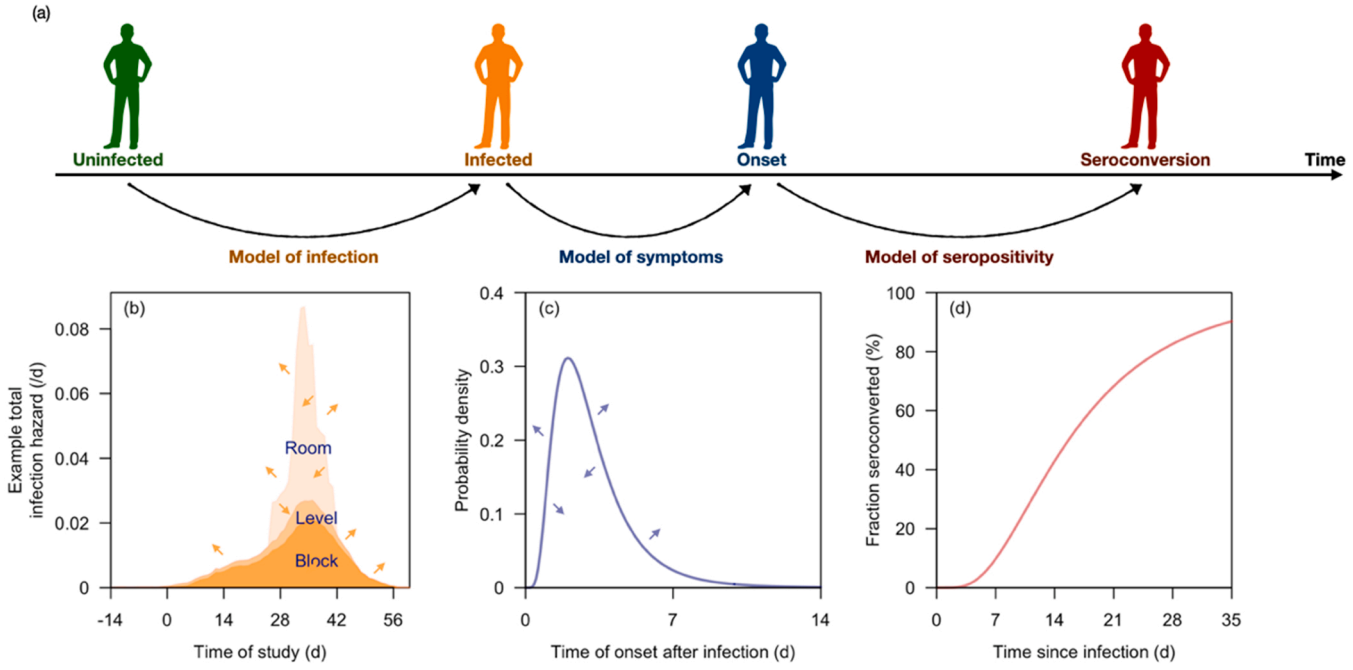

Fig. 1. Model schematic. (a) Three submodels within the overall COVID-19 transmission pathway from uninfected to seroconverted individuals. (b) Inferred total infection hazard rate for one example individual in the dormitory. Time is the time on the study (0 being the start of the trial) and the infection hazard is aggregated over the infection histories of other residents in the dormitory. (c) Inferred probability density function of incubation period length. Time is the time since infection. (d) Cumulative seroconversion rate against time since infection. Time is the time since infection. Arrows in subfigure (b) and (c) signify that the corresponding curves were to be inferred using the models rather than obtained directly from data,
whereas in figure (d), the seroconversion proportion was derived directly from the findings of Xiang et al. (2020).

$\frac{B(\alpha(t),7+\beta(t))}{B(\alpha(t),\beta(t))}$ where $B(\cdot)$ is the beta function; this formulation gives a distribution that has greater variance, but same support, as the simpler binomial distribution, and thus does not imply independence between the number of symptoms. Then, $\mathbf{P}(T^i_{onset} - T^i_{inf} = t) = \mathbf{P}(N(1) = 0) \times \mathbf{P}(N(2) = 0) \times \cdots \times \mathbf{P}(N(t-1) = 0) \times (1 - \mathbf{P}(N(t) = 0))$ and $\tau = \mathbb{E}(T^i_{onset} - T^i_{inf}) = \sum_{t=1}^{\infty} t\mathbf{P}(T^i_{onset} - T^i_{inf} = t)$..

Based on a previous meta-analysis of incubation period for COVID-19 (McAloon et al., 2020), we set the priors for this model as: $T^i_{onset} - T^i_{inf} \sim LN(log(\tau) - 0.125, 0.25), \tau \sim LN(1.88, 0.036)$ such that the mean incubation length for each individual i follows a log-normal distribution with mean τ. Thus, the posterior of the model parameters $\boldsymbol{\alpha} = (a_1, a_2, a_3, \theta)$ can be written as

$$\mathbf{P}\left(\boldsymbol{\alpha}|, \boldsymbol{N}_{sym}, \widetilde{\boldsymbol{T}}_{onset}, \widetilde{\boldsymbol{T}}_{inf}\right) \propto \left\{\prod_i \left[\prod_j \mathbf{P}\left(N^i_{sym}(t_j)\middle|, T^i_{onset} - T^i_{inf}, \tau\right)\right] \mathbf{P}\left(T^i_{onset} - T^i_{inf}\middle|, \tau\right)\right\} p(\tau),$$

where $\boldsymbol{N_{sym}} = \left\{N^i_{sym}(t_j)\right\}_{i,j}$ represents the daily number of symptoms for each infected individual considered, $\widetilde{\boldsymbol{T}}_{\boldsymbol{onset}} = \left\{T^i_{onset}\right\}_i$ the symptom onset times and $\widetilde{\boldsymbol{T}}_{\boldsymbol{inf}} = \{T^i_{inf}\}_i$ infection times.

2.4.2. Model of infection

Since we considered it unlikely for workers in different blocks to contact each other physically due to the monitoring of the dormitory, under a discrete-state continuous-time susceptible-infectious-removed (SIR) model, the infection rate at time t for individual j in the susceptible compartment was set to be

$$\lambda_j(t) = \beta_1 I^j_{block}(t) + \beta_2 I^j_{floor}(t) + \beta_3 I^j_{unit}(t),$$

where β_1, β_2 and β_3 are fixed transition rates and $I^j_{block}(t), I^j_{floor}(t), I^j_{unit}(t)$ are the number of the infectious individuals that stay in the same block, floor and unit as individual j at time t respectively.

Let $\Sigma_i(t) = \{S_i(t), I_i(t), R_i(t)\}$ be the state for individual i at time $t \in [t_{start}, t_{end}]$, here t_{start} and t_{end} are the two ends of the inference window, binary random variables $S_i(t), I_i(t), R_i(t) \in \{0,1\}$ and $S_i(t) + I_i(t) + R_i(t) \equiv 1$. When the man is susceptible, $S_i(t) = 1$; when he is infected, $S_i(t) = 0, I_i(t) = 1$; and after he recovers, $S_i(t) = I_i(t) = 0$, $R_i(t) = 1$. For each individual i, $I^i_{block}(t), I^i_{floor}(t), I^i_{unit}(t)$ is equal to the sums of the infected state $I_i(t)$'s of the persons who live in the same block, level and unit as him at time t.

Therefore, the probability that an individual becomes infected at time t given the history of the infection process $I_i(s) = \{I^i_{block}(s), I^i_{floor}(s), I^i_{unit}(s)\}$ up to time t is

$$\mathbf{P}\left(T^i_{inf} = t \middle| \{I_i(s)\}_{s\in[t_{start},\ \ t_{end}]}\right) = \lambda_i(t-)\exp\left(-\int_{t_{start}}^{t}\lambda_i(s)ds\right),$$

where $\lambda_i(t-) = \lim_{t_0 \uparrow t}\lambda_i(t_0)$ is the infection rate of individual i. In addition, if someone remains uninfected throughout the trial, i.e. he remains uninfected until time t_{end}, then the corresponding probability is

$$\mathbf{P}\left(T^i_{inf} > t_{end} \middle| \{I_i(s)\}_{s\in[t_{start},\ \ t_{end}]}\right) = \exp\left(-\int_{t_{start}}^{t_{end}}\lambda_i(s)ds\right).$$

We set the recovery time for an infected individual to be 10 days post infection (Anon, 2020) and we assigned a non-informative uniform prior for $(\beta_1, \beta_2, \beta_3)$. Thus, the posterior distribution for parameters $\boldsymbol{\beta} = (\beta_1, \beta_2, \beta_3)$ can be written as

$$\mathbf{P}(\boldsymbol{\beta}|, \boldsymbol{T_{inf}}) \propto \prod_i \left[1_{T^i_{inf} \le t_{end}}\lambda_i\left(T^i_{inf}-\right)\exp\left(-\int_{t_{start}}^{T^i_{inf}}\lambda_i(s)ds\right) + 1_{T^i_{inf} > t_{end}}\exp\left(-\int_{t_{start}}^{t_{end}}\lambda_i(s)ds\right)\right],$$

where $\boldsymbol{T_{inf}} = \boldsymbol{T^i_{inf}}\boldsymbol{i}$ are the infection times of all individuals involved.

Although the dormitory had isolation facilities for identified cases (Seet et al., 2021), the majority of the symptomatic infections were not isolated due to space constraints and some who were tested positive in PCR tests and relocated were not explicitly included in the study. Therefore, all the 4257 participants were considered in this model and the model below.

2.4.3. Model of seroprevalence

Assume $h^i(t)$ represents the SARS-CoV-2 antibody test result for individual i at time t, which equals to 1 if the result is positive and 0 otherwise, then

$$h^i(t) = 1_{t>T^i_0},$$

where $T^i_0 \ge T^i_{inf}$ is the threshold time for individual i to turn from seronegative to seropositive.

Based on the findings of Xiang et al. (2020), we assumed that the time from infection to seroconversion for individual i, ΔT^i, follows a log-normal distribution whose logarithm has a mean equal to 2.75 and standard deviation 0.62, i.e. $\Delta T^i \sim LN(2.75, 0.62^2)$, which leads to a mean time to seroconversion of 19.0 days with standard deviation 13.0 days. Thus the probability that an individual i tests positive at their serology test time t is

$$\mathbf{P}\left(t > T^i_0\right) = \mathbf{P}\left(t - T^i_{inf} > \Delta T^i\right) = F_{\Delta T^i}\left(t - T^i_{inf}\right),$$

where $F_{\Delta T^i}(\bullet)$ is the cumulative density function of the distribution $LN(2.75, 0.62^2)$..

The likelihood for each serology test result of individual i at time t^i_s is therefore

$$\mathbf{P}\left(t^i_s\middle|, T^i_{inf}\right) = \left[F_{\Delta T^i}(t^i_s - T^i_{inf})\right]^{h^i\left(t^i_s\right)}\left[1 - F_{\Delta T^i}(t^i_s - T^i_{inf})\right]^{1-h^i\left(t^i_s\right)}$$

and the total likelihood contribution for all individuals is

$$\mathbf{P}(\boldsymbol{t_s}|, \boldsymbol{T_{inf}}) = \prod_i\prod_{j=1}^{2}\mathbf{P}\left(t^i_{s_j}\middle|, T^i_{inf}\right),$$

where $\boldsymbol{t_s} = \left\{t^i_{s_j}\right\}_{i,j}$ are serology test times and $\boldsymbol{T_{inf}} = \{\boldsymbol{T^i_{inf}}\}_i$ infection times of all individuals considered in this model.

Therefore, $\mathbf{P}(\boldsymbol{\alpha}, \quad \boldsymbol{\beta}|, \boldsymbol{N_{sym}}, \widetilde{\boldsymbol{T}}_{\boldsymbol{onset}}, \boldsymbol{T_{inf}})$, the joint posterior density function for the parameters of interest, is obtained by the product of the individual posterior density functions derived in the above 3 models, i.e.

$$\mathbf{P}\left(\boldsymbol{\alpha}|, \boldsymbol{N_{sym}}, \widetilde{\boldsymbol{T}}_{\boldsymbol{onset}}, \widetilde{\boldsymbol{T}}_{\boldsymbol{inf}}\right)\mathbf{P}(\boldsymbol{\beta}|, \boldsymbol{T_{inf}})\mathbf{P}(\boldsymbol{t_s}|, \boldsymbol{T_{inf}}).$$

The model was fit using a custom designed Markov chain Monte Carlo algorithm, in which the joint posterior density function was utilized to derive the acceptance rate for new proposals in Metropolis-Hastings steps. Details are in the supplementary information.

2.5. Modelling intervention scenarios

We considered how changes in the number of individuals sharing one dormitory room would affect the final infection size in the whole dormitory in outbreaks similar in transmissibility and control to COVID-19. The changes were made by altering the number of floors in each block or the number of blocks whilst keeping the number of rooms on each floor and the population ($n = 4257$) in the dormitory the same as the original data set. At the start of each simulation, we randomly assigned dormitory residents to these rooms and 50 infected individuals were placed uniformly across the blocks to seed infection. We simulated transmission events based on the posterior mean of the $\boldsymbol{\beta}$ parameters obtained in previous steps until the end of the epidemic wave. Thus, the time from the last event (either a new infection or a new recovery) to infection for a susceptible individual i, Δt^i, was assumed to follow an exponential distribution with the mean $\lambda^i(t)$, where t is the last event time and $\lambda^i(t)$ is the infection rate at time t for individual i, i.e.

$$\Delta t^i \sim Exp\left(\lambda^i(t)\right).$$

If $\lambda^i(t) = 0$, individual i will never get infected. Then the next event time is set to be

$$t + \min\left(\left\{\Delta t^i\right\}_{i\in\mathcal{I}(t)}, \left\{T^i_{recovery} - t\right\}_{\left\{i:T^i_{recovery}>t\right\}}\right),$$

where $\mathscr{S}(t)$ is the susceptible population at time t and $T^{i}_{recovery}$ is the recovery time for individual i. We performed 1000 simulations for each scenario.

2.6. Accounting for the effects of different prophylaxes

In a secondary analysis, we explicitly accounted for the trial allocation of potential prophylaxes to individual participants. In the analysis in the original publication, statistically significant reduction in risks of infection were observed in two of the arms (oral hydroxychloroquine and povidone-iodine throat spray) compared to the comparator arm (vitamin C) (Seet et al., 2021), although the effects of both were relatively modest, as reflected in the high infection rates on all five arms. Thus, to address the potential reduction in infection risk after incorporating transmission dynamics, we allowed individuals assigned to different arms of the trial to have different risks of acquiring infection. The prophylaxes include oral vitamin C (arm A), oral hydroxychloroquine (B), oral ivermectin (C), povidone-iodine throat spray (D), and combination of oral zinc and vitamin C (E); previous analyses found that arms D and B had lower infection risks. We set prophylaxis A as the reference arm, as per the trial design, and considered the efficacy ratio of the other four candidates, r_B, r_C, r_D, r_E, so that the infection rate at time t for individual j in the susceptible compartment became

$$\lambda_j(t) = \quad r_i \times (\beta_1 I_{block}(t) + \beta_2 I_{floor}(t) + \beta_3 I_{unit}(t)),$$

where $r_i \in \{r_A, r_B, r_C, r_D, r_E\}$, $r_A \equiv 1$, $\beta_1, \beta_2, \beta_3$ are fixed transition rates and $I_{block}(t), I_{floor}(t), I_{unit}(t)$ are the number of the infectious individuals that stay in the same block, floor and unit as individual i at time t respectively. In this model, therefore, the interventions affect the risk of acquiring but not transmitting infection.

Analyses were conducted in R Core Team, (2020) and C++ . To improve computational efficiency, we used C++ to calculate the likelihoods for the proposed parameters. R was then used to integrate the C++ functions and run the Metropolis Hastings algorithm with three independent chains using the rcpp package (Eddelbuettel and François, 2011). R was also used for data-cleaning, simulation and visualization using the grid package (Zhou and Braun, 2010). Details of parameter estimation are elaborated in the Supplementary Information. The code is available at https://github.com/ShihuiJin/Tuas-South-Dorm.

3. Results

We found that the basic reproduction number, R_0, for this institutional outbreak without accounting for prophylaxis measures present was 2.76 (95 % Credible Interval (CrI) 2.65–2.87) under the assumption that a dormitory room accommodates 13 individuals, 163 individuals share a floor and 1300 individuals share a block. The seroprevalence by July 17, 2020 when the trial ended was estimated to be 64.4 % (95 % CrI 64.2–64.6 %), i.e. an estimated 2743 (95 % CrI 2731–2750) of the 4257 participants in the dormitory had been infected. The estimated mean length of the incubation period (from infection to symptom onset) was 3.5 (95 % CrI 3.3–3.8) days. The contribution of within-room contacts to the overall epidemic transmissibility was 54.7 %, i.e. excluding other forms of exposure the R_0 would have been 1.51 (95 % CrI 1.40–1.62). Transmission at the block level was estimated to contribute 35.9 %, i.e. the R_0 contribution was 0.99 secondary cases per person (95 % CrI 0.86–1.13), while contacts within other rooms on the same floor only contributed 9.4 %, or 0.26 (95 % CrI 0.11–0.42) to the R_0 (Table 2).

Table 2
Transmission rates and R_0 by stratum s of shared contacts. The contributions to R_0 by stratum s are defined by $R_0^s = \beta_s N/\gamma$. They sum to the total R_0 of 2.76 (2.65–2.87).

Stratum of shared contact	Number of typical contacts within the stratum (n)	Infection rate per infected-susceptible pair, per day (β_s, 95 %CrI)	Contribution to R_0 (95 %CrI)
Unit	13	0.012 (0.011–0.013)	1.51 (1.40–1.62)
Floor	163	0.00016 (0.00007–0.0003)	0.26 (0.11–0.42)
Block	1300	0.000076 (0.00007–0.00009)	0.99 (0.86–1.13)

The prevalence differed between blocks in the dormitory throughout the trial (Fig. 2, **SI** Table S2). Infections varied from 33.4 % (95 % CrI 31.9–34.6 %) becoming infected and 40.2 % eventually seropositive (95 % CrI 39.8–40.8 %) as of July 17, 2020 in the least affected block to 79.6 % (95 % CrI 78.7–80.1 %) becoming infected as of July 17, 2020 with a seroconversion rate of 72.9 % (95 % CrI 71.2–74.3 %) in the most affected one. The outbreaks in the five blocks were also asynchronous, with peaks observed in two blocks at the end of the first week—when 17.7 % (95 % CrI 15.3–20.1 %) and 10.6 % (95 % CrI 9.4–11.8 %) were infectious, respectively—while the peak did not occur in two others until the end of week 5 when 20.1 % (95 % CrI 18.2–22.1 %) and 29.1 % (95 % CrI 27.0–31.6 %) were infectious, respectively.

In simulations of the outbreak sizes in dormitories with different configurations (Fig. 3, **SI** Table S7), the prevalence by the end of the epidemic wave was 59 % (95 % CrI 28–64 %) if the dormitory had five 9-floor residential building blocks, which we used as a baseline for comparison. When adding one floor to each of the 5 blocks, and reducing the number of men per room accordingly, the prevalence was modelled to drop to 52 % (95 % CrI 41–57 %). The average decrease in seroprevalence caused by the addition of one floor was not linear, gradually decreasing from 7 % down to 2 % up to 18 floors. The addition of 5 floors, which reduces the density within each room by a third, causes an approximate halving in seroprevalence. By contrast, when adding one block, making a total of 6 blocks, while fixing the number of floors in each block at 9, seroprevalence decreased to 30 % (95 % CrI 17–40 %). Seroprevalence halved again, reaching 13 % (95 % CrI 5.8–21 %), when another block was added. The decline per additional block decreased to an equilibrium of ~2 % at 12 blocks or more, at which point the density within each room is close to a third of the current level.

The preceding results did not account for any differential effects of the five potential prophylaxes, and incorporating the interventions did not change the findings on the spatio-temporal spread substantially (**SI** Table S9–S10).

4. Discussion

As in many countries, the impact of Singapore's outbreak of COVID-19 was, over the first year, inequitably distributed among the population. The local epidemic was marked by large, concurrent outbreaks among migrant workers living in dormitories across the island (Yi et al., 2021). While the nascent outbreak in the general population was brought under control through lockdown measures (MOH, 2021; Dickens et al., 2020) including removal of contacts to designated quarantine facilities and isolation of all infected individuals in hospital, these measures were viewed as being impractical in controlling spread in the dormitories due to the sheer number of individuals infected. By the time the national lockdown was lifted and workers were allowed to return to work but not elsewhere in July and August 2020, around 60 % of all residents either had had a positive PCR test or were positive on serology (Tan et al., 2021). The dormitory we studied had similar outcomes, despite the prophylaxes we trialled, with partially synchronised outbreaks across the five blocks in the complex even though lockdown measures were in place. From the baseline serology, and inferred epidemic dynamics, by the time the study started, SARS-CoV-2 had already reached all buildings in the complex. The attack rates observed in these populations are comparable to homeless shelters and refugee camps (Roederer et al., 2021), and far greater than community seroprevalence studies, e.g. in California (Bendavid et al., 2021), Wuhan (Li

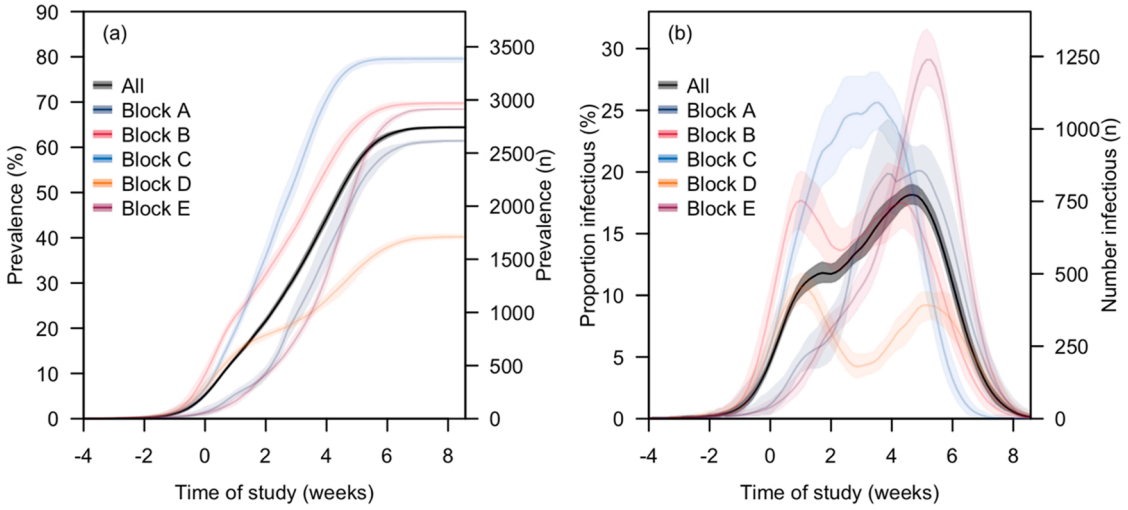

Fig. 2. Estimated proportion and number of (a) cumulative prevalence, and (b) infectious individuals overall and in each of the five blocks over an 88-day period, from 4 weeks before the trial started (April 21, 2020) to the time the trial ended (July 17, 2020). The numeric y-axes (right) are for the total across all blocks.

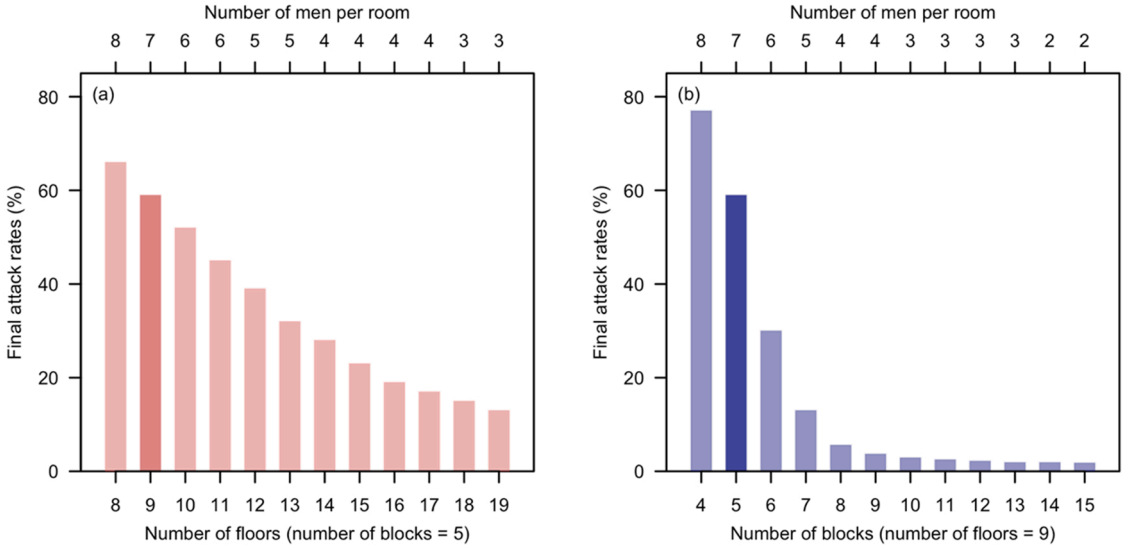

Fig. 3. Simulated outbreak size by changing numbers of a) floors; b) blocks for a fixed population. The number of men per room is the rounded average. The configuration at Tuas South Dormitory is marked with darker shades. Attack rates are average proportion from repeat Monte Carlo sampling.

et al., 2021) and Spain (Pollán et al., 2020), and by the end of 2020, there were over 20 times more PCR-confirmed cases among migrant workers in Singapore than the general population.

Several aspects of Singapore's response to the dormitory outbreaks were justifiable. These include the redeployment of healthcare workers from hospitals to provide medical care on-site (Yi et al., 2021) and to identify individuals who would require transfer to hospital for impatient care. This resulted in a very low number of deaths and need for intensive care use in the migrant worker population (Koh, 2020) which was comparable to similar aged healthy populations worldwide. While *cordons sanitaires* was effective in preventing spillover of infection back into the general population which was the ultimate goal of the approach. However, the length of lockdown in crowded conditions, and restrictions that lasted over a year on their social activities and freedom to go to third places beyond their work or home, had been reported to have a deleterious effect on their mental well-being (Saw et al., 2021).

It is therefore of public health importance that the migrant worker population and their living environments are 'future proofed', to enhance their resilience to other infectious disease outbreaks and future waves of new variants of SARS-CoV-2 or other respiratory pathogens without the same adverse consequences. While efforts are underway to provide migrant workers in Singapore with better access to healthcare through a network of dedicated primary care clinics, structural changes to their dense living environment will be needed to prevent rapid spread of pathogens. We found that, in spite of restrictions imposed on the residents when the dormitory was gazetted as an isolation area, the contribution of cross-block infections to the basic reproduction number was substantial, and indeed there was more of an overall contribution to infection risk from others in the block than from others residing on the same level of the block, due to the greater numbers of residents. This signifies the importance of contacts between workers in different rooms, possibly reflecting undetected mingling by residents despite the careful monitoring of the complex. During the outbreak, guards were posted at the entrances to each block to prevent intermingling, and although some mixing between blocks might have occurred when residents visited the clinic or store, such visits were rare with controlled timing and hence unlikely to have led to the degree of inter-block spread implied by our results. However, another hypothesis, that our data do not permit us to

assess, is that longer-distance spread of aerosols between blocks occurred, for instance as residents communicated through open windows (which was possible for some blocks but not others and not proscribed). There are no data on the potential role of environmental contamination either although Singapore has reported transmission in a public housing block detected through wastewater surveillance, this has not been reported in the dormitories (Wong et al., 2021). Similar long distance spread within residential complexes have been observed since the first SARS coronavirus outbreak (Li et al., 2005), as well as during the COVID-19 pandemic (Kwon et al., 2020; Anderson et al., 2020). If long-distance peri-domestic spread is indeed the cause of the large degree of cross-block transmission estimated here, it confirms our observation that lockdowns like those implemented in Singapore's dormitories will not prevent within complex spread, though they may prevent spread beyond the *cordon sanitaire*. If so, reducing the density of the living environment to allow social distancing during quarantines may be more effective.

Through simulations based upon the estimates from our study, we found that halving the density would have a substantial impact on the eventual prevalence under social distancing measures similar to those implemented during this study. It is worth noting that such a reduction would still lead to high-density living arrangements compared to the norm in high-income countries. One issue experienced during Singapore's foreign worker outbreaks was the lack of space for quarantine of exposed residents and isolation of cases, which was partially alleviated by converting other buildings into temporary quarantine and isolation facilities. While this was not addressed explicitly by our simulations, reducing the density of regular living arrangements would permit more flexibility in creating temporary accommodation on-site to establish cohorting of exposed and infected individuals. The strategy of aggressive contact tracing, strict isolation of cases and quarantine of all significant contacts was highly effective for the prevention of local transmission outside the dormitories during this time period.

Strengths of the study include the high participation rate of residents in the trial and the well characterised population structure. That data collection took place within the context of a clinical trial meant there were good diagnostics—with almost all participants having two serological samples bracketing the study period, suspect cases being PCR-confirmed, and moderately high self-reporting of symptoms. In addition, because the complex had been subject to public health measures by the government, there was, we believe, high compliance to restrictions on mobility within and beyond the dormitory.

Furthermore, to account for the heterogeneity in proximity between the residents, we allowed infection rates to differ for residents in a different room of the same floor, and of a different floor of the same block, while assuming a uniform transmission rate from the source to two individuals residing in the same floor but different rooms, or in the same block but different floors, which adds some flexibility compared to a fixed functional form.

Nevertheless, there are limitations worth highlighting. Not all residents participated in the trial, and for ethical reasons no data was available on them. However, because we allowed the generation time distribution to be fit to the data, their omission may not have a substantial impact on the inferences. Because the trial was conducted during a period of hard lockdown when residents were banned from leaving the dormitory except for medical care, the estimates do not reflect the situation when residents are subject to less onerous restrictions, and the specific arrangement of the dormitory, with *en suite* toilets, may make it an imperfect representation of outbreaks in dormitories with common bathing facilities. Furthermore, the study period coincided with a trial of prophylaxes, which may lower the infection rates relative to a population without such interventions, though the high attack rates on all five arms albeit reduced in two of them suggests this may not be a major limitation. We also did not have access to molecular typing data to confirm the actual transmission pathways and did not screen vendors, security personnel, healthcare workers or other individuals who may have been involved in some of the transmission pathways. Finally, although our study supports a policy of reducing the density of dormitories to increase residents' resilience to infectious disease outbreaks, the trade-off between reduced density and increased costs will need to be taken into consideration in solving this policy question.

Despite these limitations, the study sheds light on the spatio-temporal spread within a highly monitored, closed population, and casts doubt on the ability to prevent spread within such an environment through lockdown measures alone. If implementing a *cordon sanitaire* around such a population during future outbreaks, policy makers may consider allowing more freedoms within the cordon to protect residents' mental wellbeing.

CRediT authorship contribution statement

Shihui Jin: Methodology, Software, Writing – original draft, Writing – review & editing, Visualization. **Borame Lee Dickens:** Methodology, Writing – review & editing. **Amy ML Quck:** Investigation, Data curation, Writing – review & editing. **Mikael Hartman:** Investigation, Data curation, Writing – review & editing. **Paul Anantharajah Tambyah:** Investigation, Data curation, Writing – review & editing. **Raymond Chee Seong Seet:** Conceptualization, Investigation, Data curation, Writing – review & editing. **Alex R Cook:** Conceptualization, Supervision, Writing – review & editing.

Conflicts of interest

Dr Tambyah has received grants from Johnson and Johnson, GlaxoSmithKline and Roche.

Data Availability

Data will be made available on request.

Appendix A. Supporting information

Supplementary data associated with this article can be found in the online version at doi:10.1016/j.epidem.2022.100617.

References

Shadmi, E., Chen, Y., Dourado, I., Faran-Perach, I., Furler, J., Hangoma, P., et al., 2020. Health equity and COVID-19: global perspectives. Int J. Equity Health [Internet] 19 (1), 104. https://doi.org/10.1186/s12939-020-01218-z.

Team, V., Manderson, L., 2020. How COVID-19 reveals structures of vulnerability. Med Anthr. 39 (8), 671–674. https://doi.org/10.1080/01459740.2020.1830281.

Alali, W.Q., Bastaki, H., Longenecker, J.C., Aljunid, S.M., AlSeaidan, M., Chehadeh, W., et al., 2021. Seroprevalence of SARS-CoV-2 in migrant workers in Kuwait. J. Travel Med. 28 (2), taaa223. https://doi.org/10.1093/jtm/taaa223.

Gorny, A.W., Bagdasarian, N., Koh, A.H.K., Lim, Y.C., Ong, J.S.M., Ng, B.S.W., et al., 2021. SARS-CoV-2 in migrant worker dormitories: geospatial epidemiology supporting outbreak management. Int J. Infect. Dis. 103, 389–394 (Available from). ⟨https://www.ijidonline.com/article/S1201-9712(20)32457-7/abstract⟩.

Rojanaworarit, C., Bouzaidi, S.E., 2021. International labour trafficking: a neglected social origin of COVID-19. Lancet Reg. Health – West Pac. 8, 100121. ⟨https://www.thelancet.com/journals/lanwpc/article/PIIS2666-6065(21)00030-4/fulltext⟩.

Koh, D., 2020. Migrant workers and COVID-19. Occup. Environ. Med. 77 (9), 634–636. ⟨https://oem.bmj.com/content/77/9/634⟩.

Tan, I.B., Tan, C., Hsu, L.Y., Dan, Y.Y., Aw, A., Cook, A.R., et al., 2021. Prevalence and outcomes of SARS-CoV-2 infection among migrant workers in Singapore. JAMA 325 (6), 584–585. https://doi.org/10.1001/jama.2020.24071.

Sadarangani, S.P., Lim, P.L., Vasoo, S., 2017. Infectious diseases and migrant worker health in Singapore: a receiving country's perspective. J. Travel Med. 24 (4), tax014. https://doi.org/10.1093/jtm/tax014.

Franco-Paredes, C., Jankousky, K., Schultz, J., Bernfeld, J., Cullen, K., Quan, N.G., et al., 2020. COVID-19 in jails and prisons: a neglected infection in a marginalized population. PLoS Negl. Trop. Dis. 14 (6), e0008409. ⟨https://journals.plos.org/plosntds/article?id=10.1371/journal.pntd.0008409⟩.

Yi, H., Ng, S.T., Farwin, A., Pei Ting Low, A., Chang, C.M., Lim, J., 2021. Health equity considerations in COVID-19: geospatial network analysis of the COVID-19 outbreak in the migrant population in Singapore. J. Travel Med. 28 (2), taaa159. https://doi.org/10.1093/jtm/taaa159.

Chia, P.Y., Xiang Ong, S.W., Chiew, C.J., Ang, L.W., Chavatte, J.M., Mak, T.M., et al., 2021. Virological and serological kinetics of SARS-CoV-2 Delta variant vaccine-breakthrough infections: a multi-center cohort study. Clin. Microbiol Infect. (Available from) ⟨https://www.sciencedirect.com/science/article/pii/S1198743×21006388⟩.

Pulliam, J.R.C., Schalkwyk, C., van, Govender, N., Gottberg, A., von, Cohen, C., Groome, M.J., et al., 2021. Increased risk of SARS-CoV-2 reinfection associated with emergence of the omicron variant in South Africa. Science. Dec [cited 2021 Dec 20] p. 2021.11.11.21266068. Available from: ⟨https://www.medrxiv.org/content/10.1101/2021.11.11.21266068v2⟩.

COVID-19 Situation Report [Internet]. [cited 2021 Aug 30]. Available from: ⟨https://covidsitrep.moh.gov.sg/⟩.

Seet, R.C.S., Quek, A.M.L., Ooi, D.S.Q., Sengupta, S., Lakshminarasappa, S.R., Koo, C.Y., et al., 2021. Positive impact of oral hydroxychloroquine and povidone-iodine throat spray for COVID-19 prophylaxis: an open-label randomized trial. Int J. Infect. Dis. 106, 314–322 (May).

Xiang, F., Wang, X., He, X., Peng, Z., Yang, B., Zhang, J., et al., 2020. Antibody detection and dynamic characteristics in patients with Coronavirus disease 2019. Clin. Infect. Dis. Publ. Infect. Dis. Soc. Am. 71 (8), 1930–1934. Nov 5.

McAloon, C., Collins, Á., Hunt, K., Barber, A., Byrne, A.W., Butler, F., et al., 2020. Incubation period of COVID-19: a rapid systematic review and meta-analysis of observational research. BMJ Open 10 (8), e039652. Aug 16.

Anon. Position Statement from the National Centre for Infectious Diseases and the Chapter of Infectious Disease Physicians, Academy of Medicine, Singapore: Period of Infectivity to Inform Strategies for De-isolation for COVID-19 Patients. [Internet]. 2020 [cited 2021 Nov 3]. Available from: ⟨https://scholarbank.nus.edu.sg/handle/10635/168938⟩.

R Core Team. R: A Language and Environment for Statistical Computing. 2020; Available from: ⟨https://www.R-project.org/⟩.

Eddelbuettel, D., François, R., 2011. **Rcpp**: seamless *R* and *C++* integration. J. Stat. Softw. [Internet] 40 (8) (Available from). ⟨http://www.jstatsoft.org/v40/i08/⟩.

Zhou, L., Braun, W.J., 2010. Fun with the R grid package. J. Stat. Educ. 18 (3), 7 (Nov).

MOH | Updates on Singapore's COVID-19 Situation [Internet]. [cited 2021 Sep 28]. Available from: ⟨https://www.moh.gov.sg/covid-19⟩.

Dickens, B.L., Koo, J.R., Lim, J.T., Park, M., Quaye, S., Sun, H., et al., 2020. Modelling lockdown and exit strategies for COVID-19 in Singapore. Lancet Reg. Health West Pac. 1, 100004 (Available from). ⟨https://www.sciencedirect.com/science/article/pii/S2666606520300043⟩.

Roederer, T., Mollo, B., Vincent, C., Nikolay, B., Llosa, A.E., Nesbitt, R., et al., 2021. Seroprevalence and risk factors of exposure to COVID-19 in homeless people in Paris, France: a cross-sectional study. Lancet Public Health 6 (4), e202–e209 (Available from). ⟨https://www.sciencedirect.com/science/article/pii/S2468266721000013⟩.

Bendavid, E., Mulaney, B., Sood, N., Shah, S., Bromley-Dulfano, R., Lai, C., et al., 2021. COVID-19 antibody seroprevalence in Santa Clara County, California. Int J. Epidemiol. 50 (2), 410–419. https://doi.org/10.1093/ije/dyab010.

Li, Z., Guan, X., Mao, N., Luo, H., Qin, Y., He, N., et al., 2021. Antibody seroprevalence in the epicenter Wuhan, Hubei, and six selected provinces after containment of the first epidemic wave of COVID-19 in China. Lancet Reg. Health West Pac. 8, 100094 (Available from). ⟨https://www.sciencedirect.com/science/article/pii/S2666606521000031⟩.

Pollán, M., Pérez-Gómez, B., Pastor-Barriuso, R., Oteo, J., Hernán, M.A., Pérez-Olmeda, M., et al., 2020. Prevalence of SARS-CoV-2 in Spain (ENE-COVID): a nationwide, population-based seroepidemiological study. Lancet [Internet] 396 (10250), 535–544 (Available from). ⟨https://www.sciencedirect.com/science/article/pii/S0140673620314835⟩.

Saw, Y.E., Tan, E.Y., Buvanaswari, P., Doshi, K., Liu, J.C., 2021. Mental health of international migrant workers amidst large-scale dormitory outbreaks of COVID-19: A population survey in Singapore. J. Migr. Health 4, 100062 (Available from). ⟨https://www.sciencedirect.com/science/article/pii/S2666623521000295⟩.

Wong, J.C.C., Tan, J., Lim, Y.X., Arivalan, S., Hapuarachchi, H.C., Mailepessov, D., et al., 2021. Non-intrusive wastewater surveillance for monitoring of a residential building for COVID-19 cases. Sci. Total Environ. 786, 147419. ⟨https://www.ncbi.nlm.nih.gov/labs/pmc/articles/PMC8081581/⟩.

Li, Y., Duan, S., Yu, I.T.S., Wong, T.W., 2005. Multi-zone modeling of probable SARS virus transmission by airflow between flats in Block E, Amoy Gardens. Indoor Air 15 (2), 96–111 (Available from). ⟨https://onlinelibrary.wiley.com/doi/10.1111/j.1600-0668.2004.00318.x⟩.

Kwon, K.S., Park, J.I., Park, Y.J., Jung, D.M., Ryu, K.W., Lee, J.H., 2020. Evidence of long-distance droplet transmission of SARS-CoV-2 by direct air flow in a restaurant in Korea. J. Korean Med. Sci. 35 (46), e415 (Available from). ⟨https://synapse.koreamed.org/articles/1146254⟩.

Anderson, E.L., Turnham, P., Griffin, J.R., Clarke, C.C., 2020. Consideration of the aerosol transmission for COVID-19 and public health. Risk Anal. 40 (5), 902–907 (Available from). ⟨https://onlinelibrary.wiley.com/doi/abs/10.1111/risa.13500⟩.